ORIGINAL ARTICLE

A novel computer vision-based assessment of neutrophil chemotaxis in patients with severe infection

Yunxi Yang[1†], Lu Liu[1†], Zaiwen Guo[2†], Jiamin Huang[2], Linbin Li[2], Yiming Shao[2], Mingming Song[2], Aixiang Yang[3] & Bingwei Sun[2]

[1]School of Medicine, Jiangsu University, Zhenjiang, Jiangsu Province, China
[2]Department of Burns and Plastic Surgery, Affiliated Suzhou Hospital of Nanjing Medical University, Suzhou, Jiangsu Province, China
[3]Department of Intensive Care Medicine, Affiliated Suzhou Hospital of Nanjing Medical University, Suzhou, Jiangsu Province, China

Correspondence

B Sun, Department of Burns and Plastic Surgery, Affiliated Suzhou Hospital of Nanjing Medical University, Suzhou 215002, Jiangsu Province, China.
E-mail: sunbinwe@hotmail.com

[†]Equal contributors.

Abstract

Objectives. To evaluate the value of chemotactic function of neutrophils in patients with severe infections. **Methods.** A computer vision-based cellular chemotaxis analysis platform was established for the dynamic assessment of neutrophil chemotaxis. Fifty-three patients in the intensive care unit were eligible for the study. In parallel, 142 healthy volunteers were recruited to detect and establish the normal values for chemotactic function. Four chemotactic function indicators were determined–chemotaxis distance (CD), chemotaxis cell ratio (CCR), chemotaxis index (CI) and maximum speed of chemotaxis (V_{max}). The chemotaxis function scores (CFS) were calculated for further correlation analysis with clinical data. **Results.** The normal ranges of indicators were established as CD $\geq$ 1755.85 μm, CCR $\geq$ 3.34%, CI $\geq$ 39.63, $V_{max} \geq$ 14.63 μm min^{-1} and CFS $\geq$ 15. We found that the chemotactic function of neutrophils in patients suffering from infections was significantly impaired. The mean values of CD, CCR, CI, V_{max} and CFS were 1452.8 μm ($P < 0.0001$), 3.1% ($P < 0.0001$), 34.5 ($P < 0.0001$), 12.2 μm min^{-1} ($P < 0.0001$) and 9 ($P < 0.0001$), respectively. CD and CFS were significantly negatively correlated with the APACHE II score (rCD = -0.55, rCFS = -0.39), SOFA score (rCD = -0.68, rCFS = -0.56), procalcitonin concentration (rCD = -0.60, rCFS = -0.5) and the expression of P2RX1 (rCD = -0.76, rCFS = -0.56), respectively. **Conclusions.** CD, CCR, CI and V_{max} can well reflect the neutrophil chemotactic function in patients with severe infections. CFS systematically indicated neutrophil function and has promising clinical application prospects.

Keywords: cell chemotaxis analysis platform, chemotaxis function score, innate immune system, neutrophil, SOFA score

INTRODUCTION

The immune system is an effective defensive mechanism for resisting the invasion of foreign pathogens into the human body. It can discover and remove foreign matter, pathogenic microorganisms and other factors that cause disturbances to the internal environment.[1,2] Moreover, the immune system coordinates with other internal systems to maintain the stability of the internal environment and the equilibrium of the physiological state, playing an essential role in severe infections, tumors, cardiovascular diseases and so on.[3–5]

Innate (non-specific) immunity is an evolutionarily ancient host defence mechanism,[1,3] which can respond immediately to invading foreign pathogens and other danger signals and can even regulate adaptive (specific) immunity.[4,5] It underlies most inflammatory responses, especially in the early stages of microbial infection.[3] Neutrophils, also known as polymorphonuclear leukocytes (PMNs), are the most abundant leukocytes in the human blood. They act as the front-line defence of the body to resist the invasion of pathogens.[6,7] Upon invasion, neutrophils rapidly remove pathogens through chemotaxis, phagocytosis, degranulation, oxidative burst capacity and neutrophil extracellular trap (NET) generation.[8] Thus, neutrophils play an indispensable role in exerting normal immune function. To date, thorough monitoring means are available for patients with severe infection, including routine manual vital signs (e.g. pulse, respiration, temperature and blood pressure), haemodynamic detection and special indicators [e.g. procalcitonin (PCT), C-reactive protein (CRP) and brain natriuretic peptide (BNP)].[9] Nevertheless, there is no uncomplicated and effective index for evaluating of a patient's immune system.

Notably, the biological functions of neutrophils can reflect the state of the innate immune system. However, in clinical practice, medical workers pay more attention to the number of neutrophils than to their 'quality'. Clinicians' basic knowledge of clinicians and understanding of neutrophils are often limited to the absolute value and percentage in routine blood examinations. There are still many difficulties in accurately assessing neutrophil function. Chemotaxis of neutrophils means that neutrophils can migrate against the concentration gradient of chemoattractants and reach the infected sites to phagocytose and kill microorganisms.[10] The accurate assessment of neutrophil chemotactic function lays a foundation for comprehensively understanding the biological function of neutrophils. In our previous work published on PNAS,[11] we found that the ATP-gated cation channel P2RX1 is responsible for the stop signal in neutrophil chemotaxis. At present, no study in the critical-care domain has evaluated the utility of expression of the P2RX1 on neutrophils in patients with severe infections, for the assessment of neutrophil chemotactic function.

In this study, we focused on patients in the intensive care unit (ICU) with severe infections and accurately evaluated their neutrophil chemotactic function. We developed a platform, the 'Cell Chemotaxis Analysis Platform based on Computer Vision' (CCAP), and critically assessed the chemotactic function of neutrophils in 53 ICU patients with severe infections, using an improved agarose gel chemotactic model; and simultaneously detected the expression of P2RX1 on the surface of PMN synchronously. For the first time, we accurately reveal the dynamic changes in PMN chemotactic function in patients with severe infections and provided novel evaluation indexes and a potential biomarker for clinical treatment.

RESULTS

Patient characteristics

From April to August 2020, 108 patients were admitted to in the ICU. Among these patients, 55 were excluded because of the absence of microbiological documentation of infection (42 patients), 24-h APACHE II score < 3 (11 patients) or leukopenia $< 2 \times 10^9$ L^{-1} (two patients). Finally, 53 patients were included in the study (Figure 1). The characteristics of the patients and volunteers are summarised in Table 1. Among the 53 infected patients, 49 patients (92%) presented with pulmonary infections, 10 patients (19%) developed gastrointestinal infections, 5 (9%) had urinary tract infections, and one patient (2%) had a combined infection after valgus operations on both feet. The pathogens involved were gram-negative bacteria in 49 patients (92%), gram-positive bacteria in 21 patients (40%) and fungi in 21 patients (40%) (Supplementary table 1).
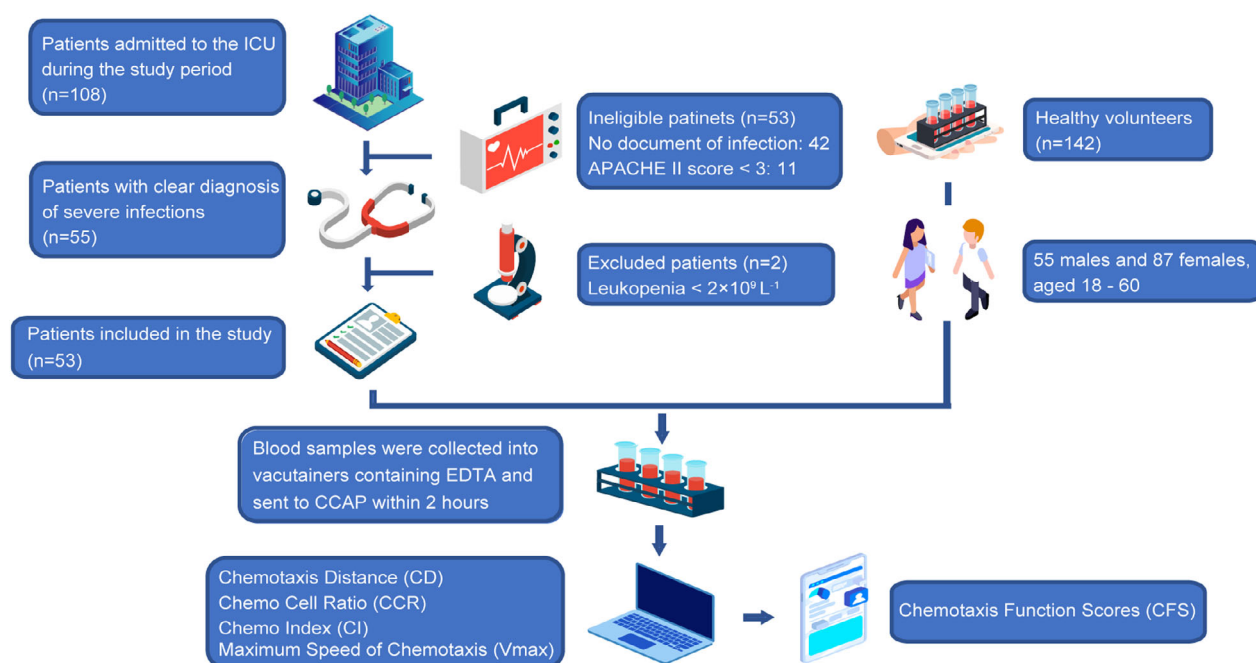
Figure 1. Flow chart of the study population.

**Table 1.** Patient demographics

Characteristic	Healthy controls (n = 142)	All patients (n = 53)	Survivors (n = 47)	Non-survivors (n = 6)	*P1-value* (Healthy controls vs all patients)	*P2*-value (Survivors vs Non-survivors)
Age, years	32 (25–35)	74 (65–82)	71 (65–82)	77 (75–81)	< 0.0001	ns
Gender, (M:F)	54:88	33:20	28:19	5:1	0.0034	ns
Neutrophil count (10^9 L^{-1})	3.5 (2.7–4.4)	7.6 (6–12.4)	7.5 (6–12)	11.4 (8.3–15.3)	< 0.0001	ns
Neutrophil percentage (%)	54.8 (50.1–60.5)	82.6 (73.6–89)	80.5 (73.1–88.3)	90.3 (90–90.4)	< 0.0001	0.0452
Lymphocyte count (10^9 L^{-1})	2.2 (1.9–2.6)	0.9 (0.6–1.3)	0.9 (0.7–1.3)	0.6 (0.6–0.8)	< 0.0001	ns
Neutrophil-to-lymphocyte ratio	1.5 (1.2–2)	9.7 (6.2–15)	8.6 (6–13)	16.8 (13–22.4)	< 0.0001	ns
Haemoglobin concentration (g L^{-1})	147.5 (132–159)	89 (78–112)	89 (77.5–109.5)	98 (82.3–119)	< 0.0001	ns
Haematocrit (%)	43.7 (40.2–46.6)	27 (23.6–33.1)	27 (23.6–32.8)	31.3 (26–37)	< 0.0001	ns
Platelet count (10^9 L^{-1})	247 (208–281)	157 (102–250)	173 (108.5–269.5)	95 (75.3–135.8)	< 0.0001	0.0132
Procalcitonin (ng mL^{-1})	–	0.3 (0.1–1.6)	0.3 (0.1–1.1)	0.7 (0.5–8.7)	–	ns
Hs-CRP (mg L^{-1})	–	40.2 (25.2–88.3)	39.3 (24.5–88.7)	53.7 (34.3–69.3)	–	ns
MOF (Y:N)	–	35:18	29:18	5:1	–	ns
APACHE II score	–	18 (15–22)	17 (15–20)	26 (24–28)	–	0.0008
SOFA score	–	5 (3–)	5 (3–6)	12 (8–15)	–	0.0002

APACHE, Acute Physiology and Chronic Health Evaluation; F, female; Hs-CRP, high-sensitivity C-reactive protein; M, male; MOF, multiple organ failure; N, no; SOFA, Sequential Organ Failure Assessment; y, year; Y, yes. Data are shown as median with interquartile range.

The normal value range of chemotactic indicator settings

A total of 142 volunteers were recruited, and their neutrophils were isolated and assessed for chemotactic function (Figure 2a), which was used to establish the normal value data of various chemotactic indicators. According to the statistical analyses described above, there were no age difference or sex differences (Figure 2c, d, f, g, i, j, l and m) in the four chemotactic indicators, and CD (Figure 2b), V_{max} (Figure 2e) and CI (Figure 2h) were all normally distributed. The CCR data did not follow a normal distribution (Figure 2k). The 95%
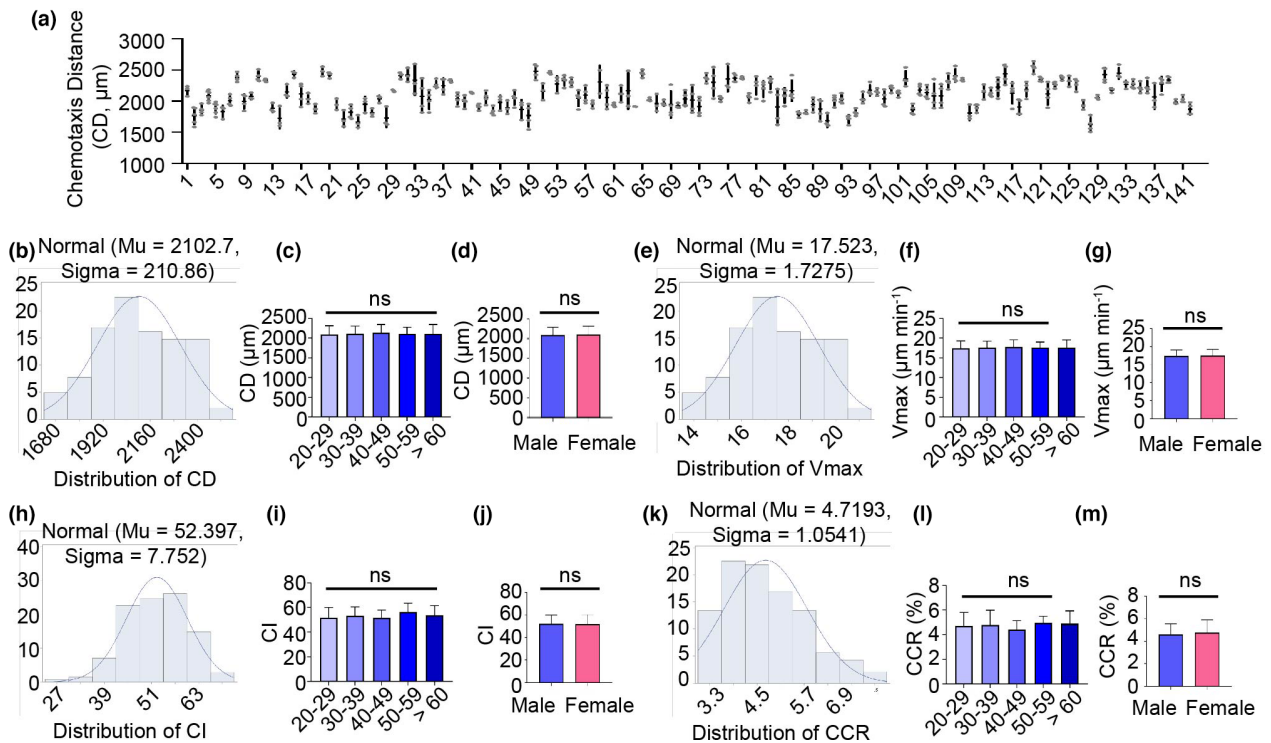
Figure 2. Normal values of four chemotactic indicators. **(a)** A summary of the CD values of neutrophils in 142 volunteers. **(b, e, f, k)** The distribution (*n* = 142) of CD **(b)**, V_{max} **(e)**, CI **(h)** and CCR **(k)**. **(c, d, f, g, i, j, l, m)** Analysis of differences between different age groups **(c, f, i, l)** and genders **(d, g, j, m)** for the four chemotactic indicators. The Kruskal–Wallis test was used to compare multiple groups and the unpaired *t*-test was used to compare the differences between pairs of groups. Mean ± standard error of the mean (SEM) SD are presented. Ns, no significance.

confidence interval was determined, and the normal range of each indicator was finally determined as follows: CD ≥ 1755.85 μm, CCR ≥ 3.34%, CI ≥ 39.63 and V_{max} ≥ 14.63 μm min^{-1}. Data below the range of these indicators were regarded as abnormalities in chemotactic function.

Circulating neutrophils were increased, but chemotactic function was decreased significantly in the infected patients

Generally, the number (Figure 3g) and percentage (Figure 3h) of circulating neutrophils were elevated in the infected patients, compared with healthy controls. However, from the intuitive CCAP analysis results, the neutrophils isolated from the infected patients presented an obvious decrease in chemotactic function (Figure 3d–f) compared with those from the healthy controls (Figure 3a–c). Additionally, through further detailed analysis of the four chemotactic indicators, each indicator of neutrophils in the infected patients was significantly lower than that of neutrophils in healthy people (Figure 3i–l). These outcomes were consistent with the results

of *in vitro* experiments (Supplementary figure 3): the chemotactic function of neutrophils was impaired by treatment with lipopolysaccharide [LPS, i.e. endotoxin, a component of the outer wall of gram-negative bacteria that sends danger signals to immune cells through Toll-like receptor 4 (TLR4)].[12] This finding suggested that although the number of neutrophils increased significantly when the patients were infected, the chemotactic function of these urgently mobilised neutrophils was extremely abnormal and could not perform their corresponding biological function of clearing invasive pathogens. The function of immune cells was inhibited, which also indicates that the function of the patient's immune system was impaired at this time.

The abnormal chemotactic function of neutrophils in infected patients was significantly correlated with the APACHE II score, SOFA score, PCT concentration and the expression of P2RX1 in PMN

Through the analysis of the chemotactic function of neutrophils in each patient, we found that the
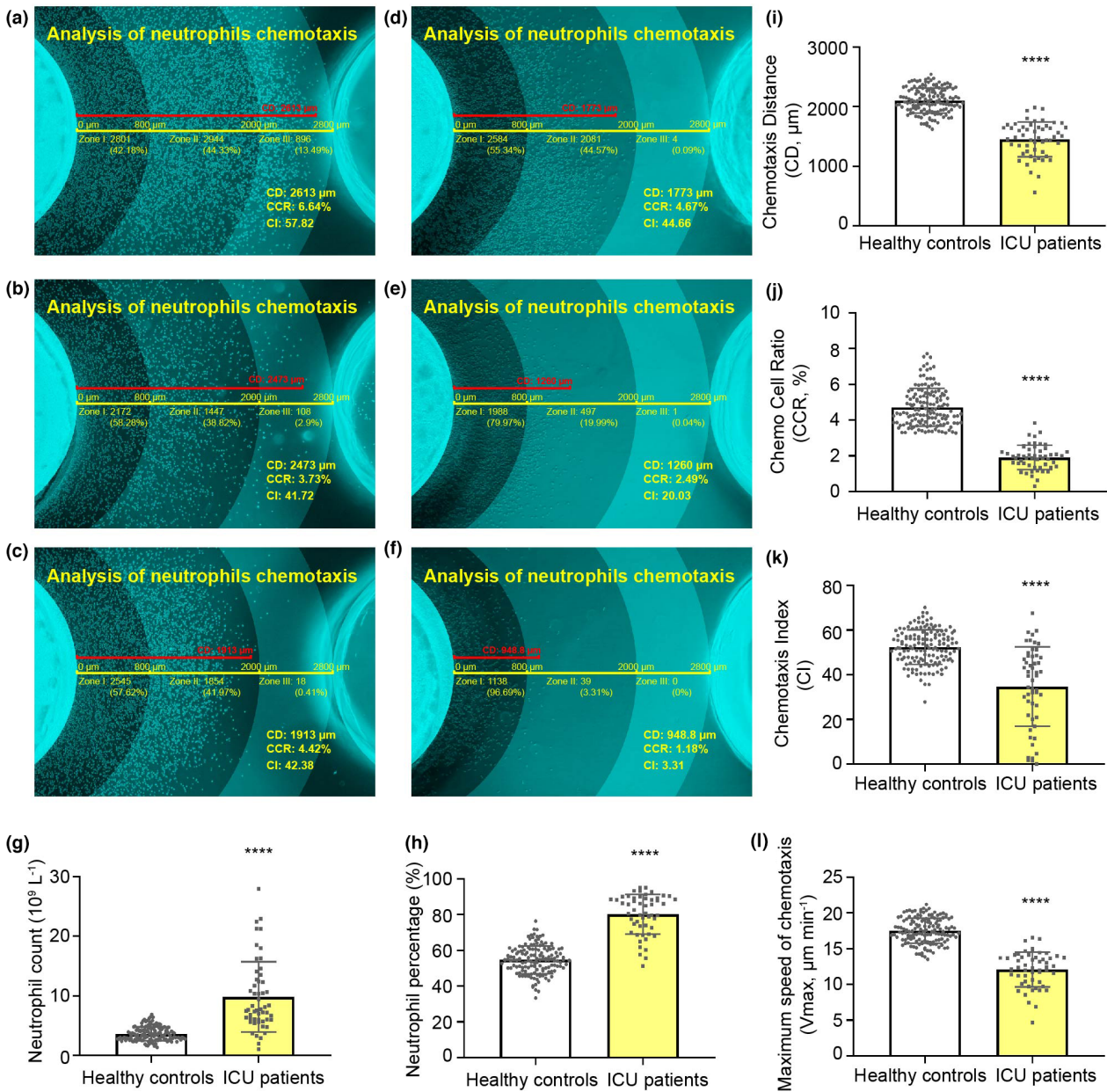
Figure 3. Infection results in the increase of number and decrease in chemotactic function of neutrophils. **(a, b, c)** Images of neutrophil chemotaxis in healthy controls: the chemotaxis were high, moderate and low, respectively. **(d, e, f)** Images of neutrophil chemotaxis in infected patients: mild infection (SOFA score < 2, APACHE II score < 9, 0.06 < PCT < 0.5 mg mL^{-1}), moderate infection (SOFA score > 2, 10 < APACHE II score < 15, 0.5 < PCT < 2 mg mL^{-1}) and severe infection (SOFA score > 2, APACHE II score > 15, PCT > 2 mg mL^{-1}). **(g, h)** Neutrophils were elevated in infected patients. **(i, j, k, l)** Neutrophil chemotactic indicators (CD, V_{max}, CI and CCR) were decreased in infected patients. An unpaired t-test was used to compare differences between pairs of groups. Mean ± standard error of the mean (SEM) SD are presented, ****P < 0.0001, compared with control group.

chemotactic function of neutrophils in most infected patients (48 patients) was impaired, but some patients (the remaining five patients) did not show obvious abnormalities (Figure 4a). Neutrophils are innate immune cells that can partially reflect the function of the immune system; therefore, we summarised the chemotactic indicators of the patients according to various classification methods (Table 2) and analysed the neutrophil chemotaxis function according to the SOFA score. Interestingly, we found that the rates of increases in the SOFA score, CD (Figure 4b),
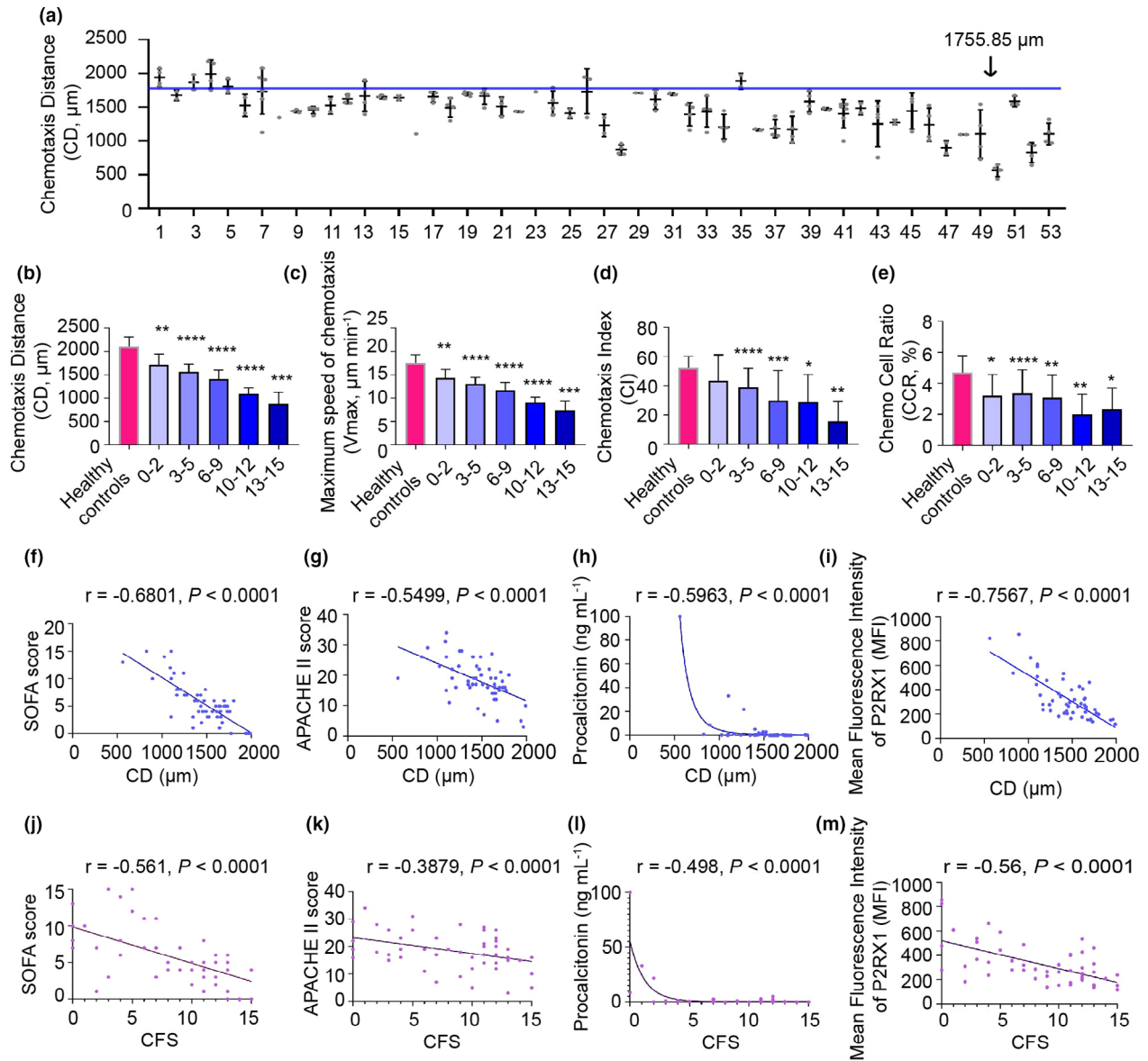
Figure 4. Chemotactic values and correlation analysis for 53 infected patients. **(a)** A summary of the CD values of neutrophils in 53 infected patients. **(b–e)** Analysis of CD **(b)**, V_{max} **(c)**, CI **(d)** and CCR **(e)** according to the SOFA score. **(f–i)** Correlation analysis between CD value and SOFA score ($r = -0.68$, $P < 0.0001$) **(f)**, APACHE II score ($r = -0.54$, $P < 0.0001$) **(g)**, PCT concentration ($r = -0.596$, $P < 0.0001$) **(h)** and the expression of P2RX1 on PMN ($r = -0.7567$, $P < 0.0001$) **(i)**. **(j–m)** Correlation analysis between CFS and SOFA score ($r = -0.56$, $P < 0.0001$) **(j)**, APACHE II score ($r = -0.39$, $P = 0.0041$) **(k)**, PCT concentration ($r = -0.5$, $P = 0.0009$) **(l)** and the expression of P2RX1 in PMN ($r = -0.56$, $P < 0.0001$) **(m)**. ANOVA was used to compare multiple groups. Mean ± standard error of the mean (SEM) SD are presented, *$P < 0.05$, **$P < 0.01$, ***$P < 0.001$, ****$P < 0.0001$, compared with control group.

V_{max} (Figure 4c) and CI (Figure 4d) gradually declined, but the trend for CCR (Figure 4e) was not obvious. Therefore, we analysed the correlations between the CD value and clinical indicators and found, surprisingly, that there were significant correlations between the CD value and SOFA score ($r = -0.68$, $P < 0.0001$) (Figure 4f), APACHE II score ($r = -0.54$, $P < 0.0001$) (Figure 4g)

and PCT concentration ($r = -0.596$, $P < 0.0001$) (Figure 4h). Interestingly, the CD value also showed a highly negative correlation with the expression of P2RX1 in neutrophils ($r = -0.7567$, $P < 0.0001$) (Figure 4i). These results indicate that the CD value can well reflect the severity of infection, the functional status of various organs and the overall condition of the patients.

Table 2. Indicators of neutrophil chemotactic function and related clinical data

	No. of patients	CD (μm)	CCR (%)	CI	V_{max} (μm min⁻¹)	Neutrophil count (10⁹ L⁻¹)	Neutrophil percentage (%)	PCT (ng mL⁻¹)
Age, years								
≤ 50	4	1800.7 (1520.2–1970.1)	3 (2.6–3.3)	35.5 (25.5–43.6)	15 (12.7–16.4)	8.4 (6.4–9.6)	79.2 (75.6–81.6)	0.2 (0.1–0.6)
51–60	4	1552.1 (1398.4–1710.8)	3.1 (2.6–3.6)	36.5 (23.6–44.4)	12.9 (11.7–14.3)	8.9 (6.8–10.5)	81.2 (75.2–86.3)	0.2 (0.1–0.2)
61–70	10	1553.8 (1279.7–1669)	2.4 (2.2–3.1)	33.3 (23.4–40.6)	12.9 (10.7–13.9)	7.7 (5.9–19)	84.1 (76–88.9)	0.5 (0.3–1.1)
71–80	18	1488.6 (1434.7–1658)	3.5 (2.6–4.9)	45.1 (39.4–49.5)	12.4 (12–13.8)	8.1 (6–15.4)	80.2 (70.8–90.3)	0.4 (0.1–2)
≥ 81	17	1346.4 (1102.2–1564.2)	2.4 (1.5–3.5)	31.2 (11.5–47.7)	11.2 (9.2–13)	7.6 (6.3–11.7)	85.7 (77.5–88.3)	0.2 (0.1–0.7)
Gender								
Male	33	1455.9 (1241.4–1696.2)	2.8 (2.2–4)	33.6 (28.1–45.4)	12.1 (10.3–14.1)	8.4 (6.9–12.7)	86.2 (77.9–89.3)	0.3 (0.1–0.6)
Female	20	1544.4 (1328.8–1624.7)	2.7 (1.8–3.7)	41.3 (11.8–47.8)	12.9 (11.1–13.5)	6.5 (5–11.1)	77.9 (67.6–86.6)	0.2 (0.1–1.8)
MOF								
No	18	1643.7 (1469.2–1762.2)	2.6 (2.3–3.8)	44.7 (29–50.6)	13.7 (12.2–14.7)	7.4 (6–13.6)	84.1 (74.8–88.5)	0.2 (0.1–0.4)
Yes	35	1409.1 (1166.8–1606.6)	3 (2.2–4.2)	33.1 (21.4–44)	11.7 (9.7–13.4)	7.7 (6–12)	80.6 (73.1–89.2)	0.3 (0.1–1.6)
APACHE II score								
0–9	5	1675.3 (1524.6–1937.1)	2.4 (1.6–1.9)	34.4 (27.1–40.9)	14 (12.7–16.1)	10.3 (8.1–21.3)	88.5 (87.4–89.2)	0.8 (0.6–1.7)
10–15	8	1650 (1498.2–1687.8)	3.1 (1.6–2.1)	45 (40.6–49)	13.8 (12.5–14.1)	6 (5.1–10)	74.8 (69.6–79.8)	0.1 (0.1–0.2)
16–20	22	1500.7 (1373.4–1651.9)	2.7 (1.2–2.4)	40.4 (21.6–48.4)	12.5 (11.4–13.8)	7.7 (6.4–13.3)	81.6 (74.2–88.3)	0.2 (0.1–0.4)
21–25	8	1441.3 (1222.7–1611)	2.4 (1.5–2.2)	41.2 (31.9–49.1)	12 (10.2–13.4)	7.2 (5.2–8.3)	79.8 (68.4–90.2)	0.3 (0.3–0.6)
26–30	8	1263.9 (1050.8–1421.5)	3.9 (1.7–2.8)	27 (9.3–37.9)	10.5 (8.8–11.8)	9.5 (6.1–13.9)	82.9 (75–90.7)	2 (0.7–6.8)
> 30	2	1098.1 (1095.2–1101)	1.3 (1.2–1.4)	27.7 (24.8–30.7)	9.2 (9.1–9.2)	11.3 (8.8–13.8)	89.2 (88.5–89.8)	16.4 (8.3–24.5)
SOFA score								
0–2	9	1675.3 (1642.2–1937.1)	2.8 (1.6–2.3)	46.9 (40.9–55.4)	14 (13.7–16.1)	8.1 (5.7–12.4)	80.5 (73.9–89.2)	0.1 (0.1–0.8)
3–5	21	1612.6 (1492.2–1659.4)	3 (1.6–2.2)	41.3 (30.1–47.7)	13.4 (12.4–13.8)	7.2 (6–9.4)	79.7 (73.6–85.7)	0.2 (0.1–0.5)
6–9	14	1397.6 (1257.9–1481.7)	2.9 (1.5–2.4)	32.1 (9.4–47.6)	11.6 (10.5–12.3)	9.4 (6.2–13.3)	85.6 (74–90.1)	1.2 (0.2–3.5)
10–12	7	1103.9 (1092.3–1135.2)	2.2 (1.1–1.5)	32 (21.9–33.6)	9.2 (9.1–9.5)	10.6 (6.3–11.7)	87.9 (86–89.3)	4.5 (0.3–14.6)
13–15	4	926 (759.3–1045.6)	2.3 (1.6–2.3)	16.2 (8.6–23.5)	7.7 (6.3–8.7)	10 (6.2–14.6)	89.4 (82.5–91)	0.7 (0.5–25.6)

CCR, chemocell ratio = (chemotactic neutrophil counts/ total number of neutrophil counts) × 100; CD, chemotaxis distance; CI, chemo index = [(cell number of zone **II**+zone **III**/total chemotactic neutrophil counts] × 100%; V_{max}, maximum speed of chemotaxis = CD/120. PCT, procalcitonin. Data are shown as median with interquartile range.

Additionally, P2RX1 provided a reasonably effective method for rapid detection of PMN chemotaxis and representation of the clinical indicators described above, owing to its high correlation with the CD value.

To more comprehensively represent the chemotactic function of neutrophils with a brief and concise index, the 'chemotaxis function score' (CFS) was established according to the range of normal values, the arrangement of abnormal values of patients and the weight of each chemotaxis index (Supplementary table 2). The CFS was graded as follows: CFS = 15 indicates normal neutrophil chemotaxis function, while < 15 indicates the opposite: 11–14 indicates mild abnormality, 7–10 indicates severe abnormality, 4–6 indicates severe abnormality, and ≤ 3 indicates extremely severe abnormality (Supplementary table 3). We graded each patient according to the CFS and analysed the correlation again. Analogously, the CFS showed a good correlation with the SOFA score ($r = -0.56$, $P < 0.0001$) (Figure 4j) and PCT concentration ($r = -0.5$, $P = 0.0009$) (Figure 4l) but showed a weak correlation with the APACHE II score ($r = -0.39$, $P = 0.0041$) (Figure 4k). Consistent with the results of CD values, CFS presented a negative correlation with the expression of P2RX1 on neutrophils also ($r = -0.56$, $P < 0.0001$) (Figure 4m). The analytical data of these correlations indicated that the expression of P2RX1 on neutrophils and chemotactic score indexes of the CFS has good prospects for clinical application; they can effectively reflect not only the chemotactic ability of neutrophils but also the severity of infection and the functional status of various organs. The highly correlated SOFA score indicates that CFS can reflect the function of the innate immune system to some extent.

Typical clinical case I

The typical clinical case I was a 65-year-old male patient with severe pulmonary infection and type 2 respiratory failure. The SOFA score was 7, the APACHE II score was 17, the CFS was 0, and the sputum culture of *Pseudomonas aeruginosa* was strongly positive on the day of admission. In terms of chronic diseases, this patient suffers from type 2 diabetes; the blood sugar is not well controlled and usually fluctuates. We performed a dynamic evaluation of PMN chemotactic function on the 1st, 2nd, 6th, 8th and 11th days after admission (Figure 5a). We found that with clinical treatment, the analysis of the four chemotactic indicators and CFS indicated that the chemotactic function of this patient recovered more with each day (the CFS changed from 0 to 15) (Figure 5b–e), which also indicated that the immune system function of the patient gradually improved. We analysed the patients' CFS and clinical indicators and discovered that with the recovery of neutrophil chemotactic function, the number of white blood cells and neutrophils gradually returned to the normal range (Figure 5f), and the blood lactic acid level gradually decreased to normal (Figure 5h). Moreover, the oxygenation index [oxygen partial pressure (PaO_2)/fraction of inspired O_2 (FiO_2)] improved (Figure 5j), the PCT level finally returned to the normal low value (Figure 5k), and pulmonary inflammation was well controlled. From the 5th day after admission, the sputum culture began to show weak positivity for *Pseudomonas aeruginosa*. However, the blood glucose concentration (Figure 5h) and haemoglobin and albumin levels (Figure 5i) of the patient did not change significantly, indicating that the CFS is insensitive to changes in nutritional status changes, and is not related to changes in body temperature (Figure 5g). The overall recovery of the patient's condition was consistent with the recovery of immune system function from PMN dynamic chemotactic function analysis. Eventually, the patient's condition improved, and she was discharged.
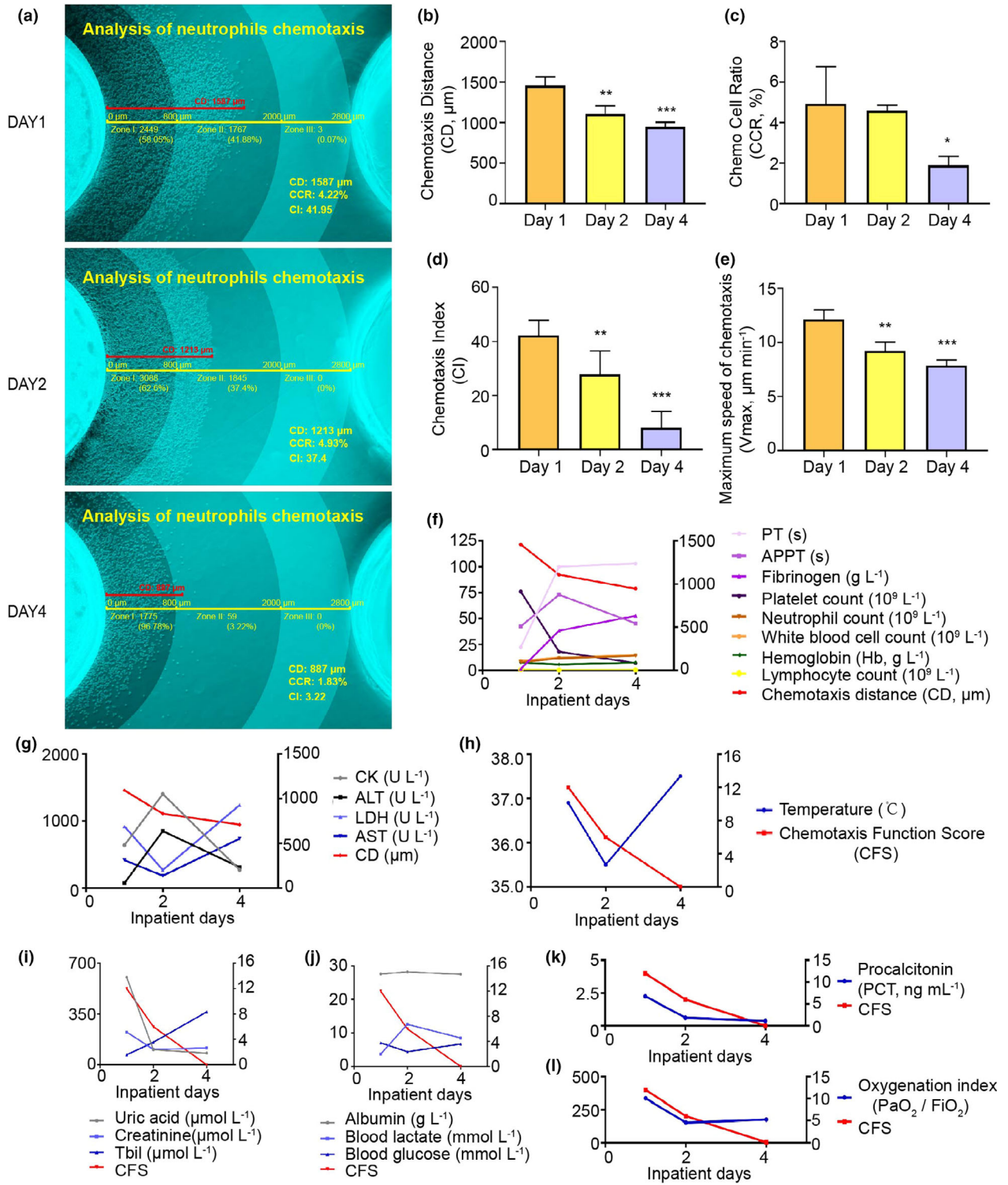
Typical clinical case II

The typical clinical case II was a 72-year-old male patient with multiple organ dysfunction (liver, kidney and blood coagulation system), pulmonary infection, and severe pleural and peritoneal effusion. The SOFA score was 7, APACHE II score was 22, the CFS was 12, and sputum culture was positive for *Klebsiella pneumoniae* on the day of admission. This patient had no history of chronic hypertension, diabetes or hyperlipidaemia. We evaluated the chemotactic function of PMNs on the 1st, 2nd and 4th day after admission (Figure 6a) and calculated the four chemotactic indicators and CFS, separately. We found that the neutrophil chemotactic function of this patient decreased daily (Figure 6b–e, Supplementary video 1), indicating that the patient's immune system gradually collapsed and was highly likely to be in a state of immunosuppression. Because of the disturbance to the liver, kidney and blood
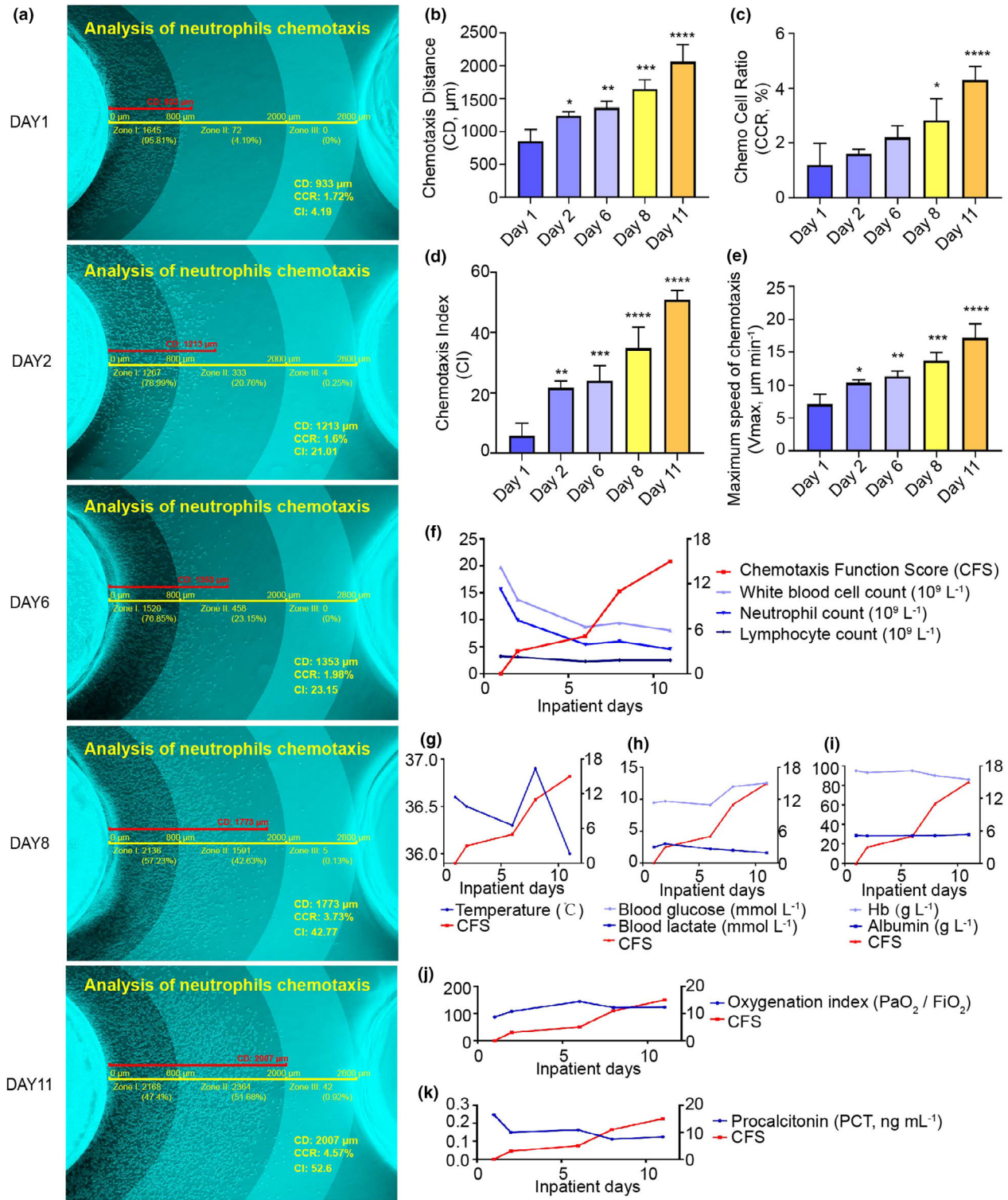
Figure 5. PMN chemotactic function assessment and clinical characteristics of case I. **(a)** General PMN chemotaxis function of patient on the 1st, 2nd, 6th, 8th and 11th day after admission. **(b–e)** Dynamic changes of four chemotactic indicators. **(f–k)** Analysis of dynamic change trend in CFS and clinical indicators. **(f)** Blood routine indexes, **(g)** body temperature, **(h, i)** nutritional status indicators, **(j)** oxygenation index and **(k)** PCT concentration. ANOVA was used to compare multiple groups. Mean ± standard error of the mean (SEM) SD are presented, *$P < 0.05$, **$P < 0.01$, ***$P < 0.001$, ****$P < 0.0001$, compared with group Day 1.

Figure 6. PMN chemotactic function assessment and clinical characteristics of case II. **(a)** General PMN chemotaxis function of patient on the 1st, 2nd and 4th day after admission. **(b–e)** Dynamic changes of four chemotactic indicators. **(f, g)** The dynamic change trend analysis of CD value with **(f)** blood routine examination and **(g)** liver function index data. **(h–l)** Analysis of dynamic change trend in CFS and other clinical indicators. **(h)** Body temperature, **(i)** indicators of liver and kidney function, **(j)** nutritional status indicators, **(k)** oxygenation index and brain natriuretic peptide (BNP) concentration and **(l)** PCT concentration. ANOVA was used to compare multiple groups. Mean $\pm$ standard error of the mean (SEM) SD are presented, $*P < 0.05$, $**P < 0.01$, $***P < 0.001$, $****P < 0.0001$, compared with group Day 1.

coagulation functions, we performed a series of analyses on the indices of total bilirubin (TB), alanine transaminase (ALT), aspartate aminotransferase (AST), creatinine, creatine kinase (CK), uric acid (UA), prothrombin time (PT) and activated partial thromboplastin time (APTT). We discovered that the number of platelets decreased daily, the platelet count was only 4×10^9 L^{-1} on the fourth day of admission, the PT and APTT had become significantly prolonged, and the international standardised ratio (INR) (Figure 6f) was significantly higher, suggesting that the function of the blood coagulation system was gradually decreasingly functional. The number of leukocytes and neutrophils remained high (Figure 6f) and the concentrations of lactate dehydrogenase (LDH), AST (Figure 6g) and TB (Figure 6i) increased significantly. Although the PCT concentration decreased (Figure 6k), the oxygenation index decreased (Figure 6l). Moreover, the sputum culture showed that *Staphylococcus haemolyticus* was positive, *Aspergillus fumigatus* grew, and the body temperature reached 37.5°C (Figure 6h) on the 4th day of admission, indicating that the patient's pulmonary infection and function had not improved. All these findings were consistent with the dynamic changes in the CFS and the previous conclusion that the patient was likely to be in a state of immunosuppression. Similarly, the patient's blood glucose, albumin (Figure 6j) and haemoglobin (Figure 6f) concentrations did not change significantly and continued to be very low. The concentrations of creatinine, UA (Figure 6i) and CK (Figure 6g) had decreased since the first day of admission, but the CK concentration was still at a significantly high level. The patient's general condition was characterised by severe multiple organ dysfunction, which could not be reversed after treatment, and the patient died.

DISCUSSION

Patients with severe infections all suffer from different degrees of immune dysfunction. Immunosuppression and infection are often interlinked, two halves of a vicious cycle that leads to organ dysfunction and even failure–common events in the ICU.[13] To date, we have already learned much about the constitution and basic functions of the immune system. With the rapid development of gene editing technology, we have made breakthroughs in the application of

acquired immune response cells to tumor treatments [for instance, 'chimeric antigen receptor T cell immunotherapy' (CAR-T)[14]], with remarkably significant results in the treatment of haematological and solid tumors.[15–17] Innate immunity generally involves innate immune cells, including PMNs, macrophages, natural killer cells (NK) and dendritic cells (DCs),[18] which play important roles in the body's response to emergency conditions, such as the recognition of and defence against microbial invasion.[19] Among them, PMNs are some of the earliest discovered innate immune cells, and their biological behaviour and function have been described in detail. However, over the last two decades, few novel discoveries on the physiological and pathophysiological aspects of PMNs have been published or reported. Clinically, antimicrobials are the primary treatment choice for patients with severe infections. However, PMNs, which can effectively treat invasive pathogenic microorganisms, have been neglected in treatment. The fact that the biological behaviour and function of PMNs in severe infections have not been well elucidated or described should not be neglected, and clinicians' knowledge (primarily, the percentage and absolute value of PMNs in routine blood reports) of PMNs remains poor.

In our previous study, we found that LPS can significantly inhibit the chemotaxis of PMNs. This indicates that the inefficiency of PMNs in effectively phagocytising and killing bacteria in patients with gram-negative bacterial infections is because of a lack of chemotaxis at the site of infection.[11] However, chemotaxis of PMNs is a hypercomplex biological process, and the methods of evaluating the chemotactic function of PMNs are very limited, such as simple agarose chemotaxis models and microfluidic chemotaxis models,[20–23] we designed an improved agarose chemotactic model and accurately defined the concentration of agarose in the model. The total number of chemotactic PMNs was set to 1×10^5, the chemotaxis direction of the PMNs was precisely controlled, and after rigorous comparative study, the chemotaxis duration of the PMNs was set to 2 hours. In this way, we obtained a unified chemotaxis diagram. On this basis, we designed and developed a novel chemotactic original diagram analysis system, CCAP. This platform is suitable for research groups. The provided RBAC permission management system makes it convenient to assign privileges to team

members, group leaders and administrators. In addition, this platform supports both PC and mobile phone systems. Bulk import and automatic processing can also be implemented, to facilitate use by researchers. Using the standard agarose chemotaxis model and CCAP mentioned above, we obtained normal PMN chemotaxis values for 142 healthy people. Normality tests were carried out for the evaluation indexes of chemotaxis (CD, CCR, CI and V_{max}), and it was confirmed that there was no sex or age difference in these indexes. The 95% confidence intervals were chosen as the reference ranges and were calculated based on the distributions. Ultimately, the normal range of chemotactic function indicators was determined: CD $\geq$ 1755.85 μm, $V_{max} \geq$ 14.63 μm min^{-1}, CI $\geq$ 39.63 and CCR $\geq$ 3.34%.

We applied the framework established above to clinical practice. We examined and evaluated the chemotactic ability of PMNs in 53 patients in the ICU. The 53 patients suffered from severe infections, multiple organ dysfunction or failure. The chemotactic distance of the PMNs in patients was significantly reduced while they presented abnormal CI, CCR and V_{max} results. Thus, the abnormal conditions of PMN chemotactic function were described based on these important parameters. Furthermore, to avoid the limitation of a single indicator of chemotaxis and to assess the chemotaxis function of PMNs quickly and accurately, we established a comprehensive PMN CFS based on the multiple chemotaxis indicators described above. We then applied it to the assessment of PMN chemotaxis in 53 patients. The results showed that the patients with the most severe infections had neutrophil chemotactic dysfunction. Concurrently, we analysed the correlations between the patient's PMN parameters and other important indexes for the same period. Interestingly, we found that the CD value and CFS were significantly correlated with the clinical SOFA score, APACHE II score and PCT concentration. Based on these correlation analyses results, we believe that various analytical indicators of PMN chemotaxis can be used as important indicators in the course of severe infections and can more accurately represent the status of the patients' innate immune system than the currently used methods. These indicators can provide clinicians with useful information; that is, in clinical practice, we should carefully examine the causes and possible mechanisms of immune system

dysfunction in patients with severe infections and the possibility of uncontrollable infections, which are closely related to immune system disorders or even dysfunction of other organs. Similarly, these indicators can also provide useful information to researchers in relevant basic clinical research, further strengthening our physiological and pathophysiological knowledge of the innate immune system—especially with regard to solving the problems arising from critical clinical diseases (such as severe infection) and diseases that are difficult to treat (such as malignant tumors), which are particularly important and urgent.

Neutrophil migration at sites of inflammation is mediated by various chemoattractant receptors, mainly the formyl-peptide receptors (FPRs), CXC chemokine receptors (CXCRs) and complement factor 5a (C5a).[24] The formyl-peptide receptor (FPR) gene cluster in humans has three members: FPR1, FPRL1 and FPR2.[25] A study on an LPS-based murine model of neuroinflammation showed that LPS administration increased the expression of the membrane fMLP receptor (FPR1).[26] Similarly, in a study on acute lung injury, Liu *et al.*[27] found that FPR2 expression was markedly increased in the lung tissues of LPS-challenged mice. Bylund *et al.*[28] showed that treatment of neutrophils with LPS at 37°C for 30 min resulted in increased the expression of membrane FPRL1. Mattos *et al.*[29] found that the expression of IL-8 receptors CXCR1 and CXCR2 on the surface of neutrophil membranes increased in several mouse models of airway inflammation, and the CXCR1/2 antagonist could reduce airway inflammation and improve lung function. Additionally, C5a plays an essential role in neutrophil migration via interaction with its receptor (C5aR). C5a could impair the chemotaxis and phagocytosis of neutrophils by downregulating the expression of C5aR-CD88.[30] These outcomes indicate that the expression of chemoattractant receptors increases in the inflammatory state and aggravates the inflammatory response through various mechanisms. Moreover, the high mobility group protein B1 (HMGB1)-mediated neutrophil migration has been reported to be critical for defending against infection.[31,32]

In recent years, the length of time before research outcomes are applied in the clinic have gradually decreased, while the concerns about neutrophils in clinical patients have gradually increased; however, most of them remain in molecular biology analysis and are not associated

with other clinical indicators. It may take a long time to implement this knowledge in clinical applications. Our research circumvents such shortcomings and connects scientific research and clinical practice. Although the results of this study have clear clinical significance, they are constrained by the small sample size and differences between the basic diseases and severity of infections in patients; thus, the impact of this study is inevitably restricted. Additionally, in terms of age and gender balance, patients with severe infections were mainly middle-aged and elderly patients, which made it difficult to recruit age-matched healthy volunteers. Therefore, the chemotactic indicators of different age segments and genders in the healthy population were analysed, and the influencing components of gender and age on the chemotactic function of neutrophils were excluded. We anticipate that with future in-depth studies on the innate immune system, the complex biological behaviour of innate immune cells under pathological conditions will be more comprehensively clarified. Additionally, that with the application of research results to clinical practice, strong theoretical guidance will be provided for the treatment of critically ill patients.

METHODS

Ethics statement

This study was approved by the Medical Ethical Committee of the Suzhou Municipal Hospital. Blood specimens were extracted from the cubital veins of healthy drug-free donors and patients. Written informed consent was obtained from all participants before their inclusion in the study. All experiments were performed in accordance with approved guidelines.

Patients and volunteers

We prospectively included all adult patients admitted to the medical ICU of the Affiliated Suzhou Hospital of Nanjing Medical University from April 2020 to August 2020, for whom neutrophil chemotactic function was assessed. Patients who were diagnosed with infections and had APACHE II scores (24 h) $\geq$ 3 were eligible for the study. Patients who were COVID-19 positive, pregnant, declared to be deprived of their liberty by judicial or administrative decisions, receiving corticosteroid treatment, bone marrow transplant patients, blood transfusion patients and with leukopenia below $2 \times 10^9 \, L^{-1}$ were excluded.

Moreover, 142 volunteers with normal physical examination result were recruited from the general population, to detect and establish the normal value of neutrophil chemotactic function.

Patients were enrolled between April 2020 and August 2020, with the last patient follow-up in October 2020. Written informed consent was obtained from volunteers, patients or the patients' legal representatives.

Data collection

For all the patients included in this study, routine blood samples taken at admission were used for the assessment of neutrophil chemotactic function; some patients also underwent dynamic blood collection and analysis. For each patient, the following data were collected: age, sex, medical history, reasons for admission, acute physiology, chronic health evaluation II (APACHE II), sequential organ failure assessment (SOFA), major diagnoses, length of stay, mortality in ICUs and laboratory results for all samples. For the volunteers, in addition to basic information, such as sex and age, the results obtained from medical examinations were also included in the statistics (Table 1).

Cell preparation

Human whole blood was obtained from healthy volunteers and patients at the medical ICU of the Affiliated Suzhou Hospital of Nanjing Medical University under an approved human ethics protocol. Neutrophils were isolated using the EasySep™ Direct Human Neutrophil Isolation Kit (STEMCELL Technologies, Canada), according to the manufacturer's instructions. Cells were suspended in RPMI-1640 (Gibco, Canada) with Ca^{2+}, Mg^{2+} and 10% foetal bovine serum (FBS) (Gibco, New Zealand) at 1.0×10^7 cells mL^{-1}.

Under-agarose neutrophil chemotaxis model

The under-agarose neutrophil chemotaxis model was established, as previously described.[14] Briefly, a 1.2% agarose solution was boiled and mixed in a 1:3 ratio with heated medium containing 50% HBSS with Ca^{2+}, Mg^{2+} and 50% RPMI 1640 (20% heat-inactivated FBS). Approximately 2.7 mL of the above-described solution was poured into a 35-mm culture dish that had been precooled to 4°C. After half an hour, the agarose gel solidified, and three wells that were 3 mm in diameter and 2.8 mm apart were cut in a straight line in the gel. The middle well was filled with 10 μL of chemoattractant fMLF (0.1 μmol, a potent chemotactic peptide of neutrophils) (Sigma Aldrich, USA), and the side wells were filled with 10 μL of neutrophils at 1.0×10^7 cells mL^{-1} (treated as indicated). Gels were incubated for 2 h in a 37°C/5% CO_2 incubator. The original patterns of neutrophil chemotaxis were observed and documented using an Olympus IX71 microscope under 4× magnification.

Construction of the Cellular Chemotaxis Analysis Platform (CCAP) based on Computer Vision66

The platform resolves the micrographs of the cells. On this basis, cellular chemotaxis was statistically analysed using

computer vision algorithms, and the report was automatically exported. The platform is user-friendly and supports the one-key analysis function. After being uploaded by users, the original cellular micrographs are automatically repaired and strengthened on the platform. Subsequently, multiple algorithms are combined to calculate and statistically analyse the graphs to obtain the cellular chemotaxis, for export. Specifically, contrast-limited adaptive histogram equalisation (CLAHE) is first used to improve the resolution of the original micrographs by image denoising and contrast enhancement. The images are further processed by grey scaling, binarisation and adhesion cutting in concentric circle mode. Statistical results are finally marked on the images for export (Supplementary figure 1). This platform is suitable for research groups. The provided RBAC permission management system makes it convenient to assign privileges to team members, group leaders and administrators. In addition, this platform supports both PC and mobile phone systems. Bulk import and automatic processing are also implemented, helpful for facilitating use by researchers.

Evaluation of neutrophil chemotaxis ability

Chemotaxis of neutrophils was observed and documented based on one-quarter of the perimeter of the holes on both sides of the micrographs using an Olympus IX71 microscope under $4\times$ magnification, and the images were uploaded to CCAP for analysis. The region of chemotaxis was divided into three zones according to the CD: Zone I (< 800 μm), Zone II (800–2000 μm) and Zone III (> 2000 μm). Additionally, the number of neutrophils in the chemotaxis region was counted automatically, and several parameters, CD, CCR, CI, and V_{max}, were set to evaluate the chemotactic function of neutrophils more comprehensively (Supplementary figure 2), where CD is chemotaxis distance, CCR is chemotactic cell ratio, CI is chemotactic index and V_{max} is the maximum speed of chemotaxis. All quantitative analysis data were obtained once uploaded and analysed and could be optionally downloaded for viewing and checking.

Assessment of expression of P2RX1 on the surface of neutrophils

To detect the expression of the neutrophil P2X1 receptor, isolated neutrophils were incubated with an anti-P2X1 receptor-FITC antibody (Alomone Labs, Israel) at $4°C$ for 1h (5 μg antibody/ 5×10^5 cells), cells were washed twice in cold PBS and analysed by using BD FACS Canto II Flow cytometry.

Statistical analysis

All statistical analyses and graphs were produced using GraphPad Prism software (version 8.0). Statistical results for continuous variables are expressed as medians and interquartile ranges (25th–75th). Student's *t*-test and Mann–Whitney *U* test were applied to compare the differences between the two groups. For group comparisons, one-way analysis of variance (ANOVA) was used for continuous

variables with a normal distribution, and the Kruskal–Wallis test was used for continuous variables with skewed distributions. The results are expressed as the mean $\pm$ standard deviation (SD), and statistical significance was set at a $P < 0.05$. The Shapiro–Wilk test was used to test the normality of the distributions of chemotaxis distance, chemotaxis cell ratio, chemotaxis index and V_{max}. The 95% confidence intervals were chosen as the reference ranges and were calculated based on the distributions. For variables with normal distributions, 95% of the measurements were within the range of 1.645 SDs for one side or within the range of 1.96 SDs for either side; for those with skewed distributions, 95% of the reference ranges were below 95% or over 5% for one side and within 2.5–97.5% for both sides.

CONCLUSIONS

This study is the first to evaluate the utility of PMN chemotactic function in the assessment of innate immune system function. Our findings show that the chemotactic function of PMNs can not only partially represent the state of the innate immune system in infected patients, but also the severity of infection and functional status of various organs. However, further studies are needed to elucidate the role of the assay for PMN chemotactic function in the diagnosis and treatment of infections in ICUs.

ACKNOWLEDGMENTS

CONFLICTS OF INTEREST

The authors declare no conflict of interest.

AUTHOR CONTRIBUTIONS

Yunxi Yang: Conceptualization; Data curation; Formal analysis; Investigation; Methodology; Project administration; Writing-original draft; Writing-review & editing. **Lu Liu:** Data curation; Formal analysis; Methodology; Project administration; Software; Writing-review & editing. **Zaiwen Guo:** Data curation; Formal analysis; Methodology; Project administration; Software; Writing-review & editing. **Jiamin Huang:** Data curation; Formal analysis; Methodology. **Linbin Li:** Data curation; Formal analysis; Methodology. **Yiming Shao:** Data curation; Investigation. **Mingming Song:** Data curation; Investigation. **Aixiang Yang:** Conceptualization; Investigation; Resources. **Bingwei Sun:** Conceptualization; Formal analysis; Funding acquisition; Project administration; Resources; Supervision; Writing-review & editing.

DATA AVAILABILITY STATEMENT

Data are available from the authors upon reasonable request.

REFERENCES

1. Hoffmann J, Kafatos F, Janeway C, Ezekowitz R. Phylogenetic perspectives in innate immunity. *Science* 1999; **284**: 1313–1318.
2. Paludan S, Pradeu T, Masters S, Mogensen T. Constitutive immune mechanisms: mediators of host defence and immune regulation. *Nat Rev Immunol* 2021; **21**: 137–150.
3. Janeway C, Medzhitov R. Innate immune recognition. *Annu Rev Immunol* 2002; **20**: 197–216.
4. Kar U, Joosten L. Training the trainable cells of the immune system and beyond. *Nat Immunol* 2020; **21**: 115–119.
5. Iwasaki A, Medzhitov R. Control of adaptive immunity by the innate immune system. *Nat Immunol* 2015; **16**: 343–353.
6. Liew P, Kubes P. The neutrophil's role during health and disease. *Physiol Rev* 2019; **99**: 1223–1248.
7. Kienle K, Lämmermann T. Neutrophil swarming: an essential process of the neutrophil tissue response. *Immunol Rev* 2016; **273**: 76–93.
8. Kolaczkowska E, Kubes P. Neutrophil recruitment and function in health and inflammation. *Nat Rev Immunol* 2013; **13**: 159–175.
9. Gros A, Roussel M, Sauvadet E *et al*. The sensitivity of neutrophil CD64 expression as a biomarker of bacterial infection is low in critically ill patients. *Intensive Care Med* 2012; **38**: 445–452.
10. Petri B, Sanz M. Neutrophil chemotaxis. *Cell Tissue Res* 2018; **371**: 425–436.
11. Wang X, Qin W, Xu X *et al*. Endotoxin-induced autocrine ATP signaling inhibits neutrophil chemotaxis through enhancing myosin light chain phosphorylation. *Proc Natl Acad Sci USA* 2017; **114**: 4483–4488.
12. Skirecki T, Cavaillon J. Inner sensors of endotoxin - implications for sepsis research and therapy. *FEMS Microbiol Rev* 2019; **43**: 239–256.
13. van der Poll T, van de Veerdonk F, Scicluna B, Netea M. The immunopathology of sepsis and potential therapeutic targets. *Nat Rev Immunol* 2017; **17**: 407–420.
14. Hong M, Clubb J, Chen Y. Engineering CAR-T cells for next-generation cancer therapy. *Cancer Cell* 2020; **38**: 473–488.
15. Mikkilineni L, Kochenderfer J. CAR T cell therapies for patients with multiple myeloma. *Nat Rev Clin Oncol* 2021; **18**: 71–84.
16. Rafiq S, Yeku O, Jackson H *et al*. Targeted delivery of a PD-1-blocking scFv by CAR-T cells enhances anti-tumor efficacy *in vivo*. *Nat Biotechnol* 2018; **36**: 847–856.
17. Reinhard K, Rengstl B, Oehm P *et al*. An RNA vaccine drives expansion and efficacy of claudin-CAR-T cells against solid tumors. *Science* 2020; **367**: 446–453.
18. Weichhart T, Hengstschläger M, Linke M. Regulation of innate immune cell function by mTOR. *Nat Rev Immunol* 2015; **15**: 599–614.
19. Napier B, Monack DM. A lipid arsenal to control inflammation. *Science* 2016; **352**: 1173–1174.
20. McMinn P, Hind L, Huttenlocher A, Beebe D. Neutrophil trafficking on-a-chip: an *in vitro*, organotypic model for investigating neutrophil priming, extravasation, and migration with spatiotemporal control. *Lab Chip* 2019; **19**: 3697–3705.
21. Kim D, Haynes C. On-chip evaluation of neutrophil activation and neutrophil-endothelial cell interaction during neutrophil chemotaxis. *Anal Chem* 2013; **85**: 10787–10796.
22. Hamza B, Irimia D. Whole blood human neutrophil trafficking in a microfluidic model of infection and inflammation. *Lab Chip* 2015; **15**: 2625–2633.
23. Heit B, Liu L, Colarusso P *et al*. PI3K accelerates, but is not required for, neutrophil chemotaxis to fMLP. *J Cell Sci* 2008; **121**: 205–214.
24. Zhang H, Sun B. Pleiotropic regulations of neutrophil receptors response to sepsis. *Inflamm Res* 2017; **66**: 197–207.
25. Gao J, Chen H, Filie J *et al*. Differential expansion of the N-formylpeptide receptor gene cluster in human and mouse. *Genomics* 1998; **51**: 270–276.
26. Calvello R, Cianciulli A, Porro C *et al*. Formyl peptide receptor (FPR)1 modulation by resveratrol in an LPS-induced neuroinflammatory animal model. *Nutrients* 2021; **13**: 1418.
27. Liu H, Lin Z, Ma Y. Suppression of Fpr2 expression protects against endotoxin-induced acute lung injury by interacting with Nrf2-regulated TAK1 activation. *Biomed Pharmacother* 2020; **125**: 109943.
28. Bylund J, Karlsson A, Boulay F, Dahlgren C. Lipopolysaccharide-induced granule mobilization and priming of the neutrophil response to Helicobacter pylori peptide Hp(2–20), which activates formyl peptide receptor-like 1. *Infect Immun* 2002; **70**: 2908–2914.
29. Mattos M, Ferrero M, Kraemer L *et al*. CXCR1 and CXCR2 Inhibition by ladarixin improves neutrophil-dependent airway inflammation in mice. *Front Immunol* 2020; **11**: 566953.
30. Conway Morris A, Kefala K *et al*. C5a mediates peripheral blood neutrophil dysfunction in critically ill patients. *Am J Respir Crit Care Med* 2009; **180**: 19–28.
31. Berthelot F, Fattoum L, Casulli S *et al*. The effect of HMGB1, a damage-associated molecular pattern molecule, on polymorphonuclear neutrophil migration depends on its concentration. *J Innate Immun* 2012; **4**: 41–58.
32. Zhang J, Li Q, Zou Y *et al*. HMGB1-TLR4-IL-23-IL-17A axis accelerates renal ischemia-reperfusion injury via the recruitment and migration of neutrophils. *Int Immunopharmacol* 2021; **94**: 107433.

Supporting Information

Additional supporting information may be found online in the Supporting Information section at the end of the article.